cogent engineering

Taylor & Francis
Taylor & Francis Group

Cogent Engineering

ISSN: (Print) 2331-1916 (Online) Journal homepage: https://www.tandfonline.com/loi/oaen20

Experimental investigation and modelling on air layer formation around a rotating grinding wheel

Sujit Majumdar, Ahin Banerjee, Santanu Das & Samik Chakroborty

To cite this article: Sujit Majumdar, Ahin Banerjee, Santanu Das & Samik Chakroborty (2016) Experimental investigation and modelling on air layer formation around a rotating grinding wheel, Cogent Engineering, 3:1, 1183273, DOI: 10.1080/23311916.2016.1183273

To link to this article: https://doi.org/10.1080/23311916.2016.1183273

Accepted author version posted online: 27 Apr 2016.
Published online: 31 May 2016.

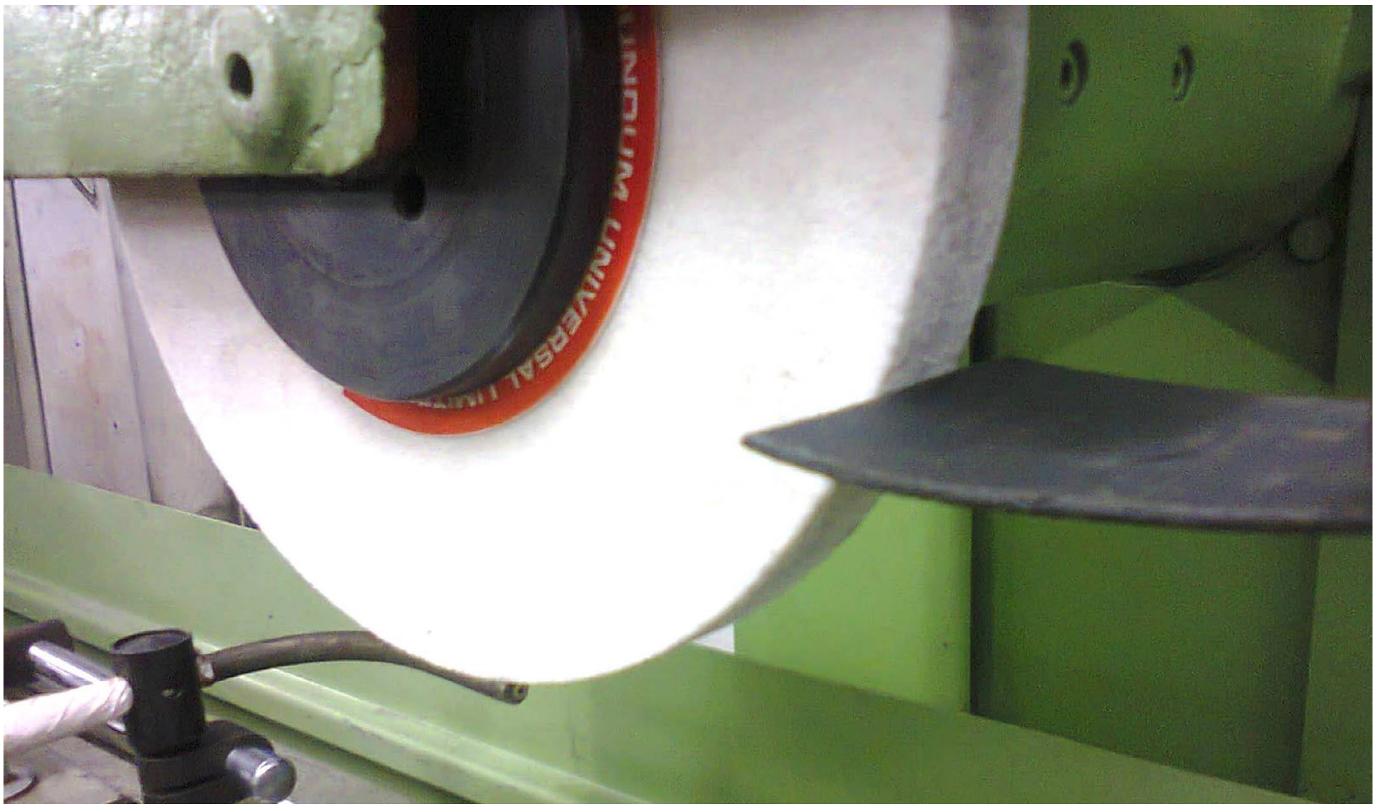

PRODUCTION & MANUFACTURING | RESEARCH ARTICLE

Experimental investigation and modelling on air layer formation around a rotating grinding wheel

Sujit Majumdar, Ahin Banerjee, Santanu Das and Samik Chakroborty

Cogent Engineering (2016), 3: 1183273

Majumdar et al., *Cogent Engineering* (2016), 3: 1183273
http://dx.doi.org/10.1080/23311916.2016.1183273

cogent engineering

PRODUCTION & MANUFACTURING | RESEARCH ARTICLE

Experimental investigation and modelling on air layer formation around a rotating grinding wheel

Sujit Majumdar[1], Ahin Banerjee[2], Santanu Das[3]* and Samik Chakroborty[4]

Received: 20 October 2015
Accepted: 24 April 2016
First Published: 27 April 2016

*Corresponding author: Santanu Das, Department of Mechanical Engineering, Kalyani Government Engineering College, Kalyani 741235, West Bengal, India
E-mail: sdas.me@gmail.com

Reviewing editor:
Zude Zhou, Wuhan University of Technology, China

Additional information is available at the end of the article

Abstract: Impingement of grinding fluid deep into grinding zone is a challenge due to presence of air layer around the grinding wheel. This paper presents experimental observation on air boundary layer formed around a rotating grinding wheel, a rexine-cloth covered grinding wheel and a solid disc. The effect of porous and rough grinding wheel surface towards strengthening air boundary layer has been studied. Modelling has been done to estimate variation of air pressure within this boundary layer. Out of three different methods of extrapolation done, the most suitable one is suggested. Results obtained using three different wheels are compared. A scraper board is also employed to observe reduction of air pressure. Higher value of air pressure is noted in case of bare grinding wheel than that in other conditions. Use of scraper board along with rexine-covered wheel is found to reduce air pressure to a large extent such that it becomes close to air pressure noted around the solid wheel. It shows the beneficial effect of using scraper board and rexine-pasted wheel to suppress air layer effectively. Correspondingly, grinding fluid is expected to reach deep into the grinding zone thereby rendering better control of grinding temperature, and hence, better grinding performance.

Sujit Majumdar

ABOUT THE AUTHORS

Sujit Majumdar has completed his MTech in Production Engineering from Kalyani Government Engineering College, Kalyani. After serving in Indian Air Force for more than a decade, he is now engaged in teaching and research at Global Institute of Management & Technology, Krishnanagar.

Ahin Banerjee is a BTech of Mechanical Engineering from West Bengal University of Technology, Kolkata. He completed MTech in Production Engineering from Kalyani Government Engineering College, Kalyani. He is now a Research Scholar at IIT (BHU), Varanasi.

Dr Santanu Das is Professor and Head of Mechanical Engineering Department, Kalyani Government Engineering College, Kalyani. He did his Bachelors and Masters from Jadavpur University, Kolkata and obtained PhD from Indian Institute of Technology, Kharagpur.

Dr Samik Chakraborty has received the MSc, MTech and PhD degree from Jadavpur University, Kolkata. In 2006, he joined Indian Maritime University as a Lecturer. He is a Senior Member of IEEE and Life Member of FOSET.

PUBLIC INTEREST STATEMENT

Grinding is done with a high speed rotating wheel for giving finishing or semi-finishing touch to a workpiece. When a wheel rotates, an air layer is formed around it. In this work, an experimental observation has been made to find out the variation of pressure of air layer formed around the wheel. This air layer obstructs the grinding fluid delivery into the wheel-workpiece interface, and hence, hampers cooling and lubrication of workpiece and wheel. First, rexine cloth is pasted on both faces of the wheel to restrict axial suction of air so that air layer pressure can be less. Next, scraper board is employed against the wheel to physically obstruct the existing air layer. Both of these techniques have been explored for effectively suppressing the air layer, such that grinding fluid can reach deep into the grinding zone. As a result, better ground product quality can be possible to make.

Subjects: Manufacturing & Processing; Manufacturing Engineering Design; Manufacturing Technology

Keywords: grinding; air boundary layer; solid disc; rexine-pasted wheel; grinding wheel; porosity; roughness; modelling

1. Introduction

Grinding is a surface finishing operation associated with high heat, surface burn, residual stress, etc. that may cause undesirable scrapping of the workpiece at its last stage (Guo & Malkin, 1992; Malkin, 1990). To prevent these ill effects, cutting fluid is introduced into the contact zone of grinding wheel and workpiece. However, conventional flood cooling is reported to be effective by only less than 30%. Only 5–30% of the quantity of fluid applied cools, or lubricates, grinding region (Guo & Malkin, 1992; Kovacevic & Mohan, 1995; Mandal, Majumdar, Das, & Banarjee, 2010, 2011). Morgan et al. (2008) have shown that a fluid discharge through nozzle results in only one quarter of it to pass through wheel-work interface. This increases overall machining cost as the cost of disposal of this working fluid may go up to 15% of total cost of manufacturing (Brinksmeir, 1993). With an increase in wheel velocity, it has been observed that power needed to provide fluid flow has to be increased as the air flow around grinding wheel increases with the increase in wheel speed (Majumdar, Mandal, Das, & Chakroborty, 2015; Nguyen & Zhang, 2006). This happens due to the hindrance imposed by air boundary layer which is formed due to the rotation of a disc or wheel in a static fluid, such as air in this case (Catai et al., 2006, 2008; Das, 2003). This investigation is an experimental observation and model development of the formation of air boundary layer around three different types of wheels and to examine the difference of boundary layer formation in order to find out the root cause of it. This may, in turn, help in finding the strategy of issuing grinding fluid into the grinding zone. It also suggests some methods to minimize this rotating air which hinders grinding fluid to reach deep into the tool-work interface.

To suppress the air boundary layer in order to improve the better delivery of grinding fluid, many methods have been applied. Use of pneumatic barrier against this flow of air around the wheel can reduce its strength by an amount of 50% (Mandal, Das, Das, & Banerjee, 2014; Mandal, Singh, Das, & Banerjee, 2011, 2012). Grindability is also found to be improved by breaking this air barrier partially by pneumatic barrier while grinding inconel 600 (Mandal, Biswas, Sarkar, Das, & Banarjee, 2013a). But the use of pneumatic barrier is costly and the effect is not much influential. Use of deflector system has been observed to eliminate such layer of air but not to a high extent (Catai et al., 2008; Das, 2003). Ramesh, Yeo, Zhong, and Sim (2001) have shown practically, coolant shoe can reduce this barrier and its effect remains up to 60° of the grinding wheel periphery after it. It has been concluded by a number of researchers that grinding performance can be improved by the control of this air layer (Akiyama, Shibata, & Yonetsu, 1984; Banerjee, Ghosal, & Dutta, 2008; Catai et al., 2008; Ebbrell, Wooly, Tridimas, Allanson, & Rowe, 2000; Han & Li, 2013; Mandal, Biswas, Sarkar, Das, & Banarjee, 2013b; Peukart, 2004; Schumack, Chung, Schultz, & Asibu, 1991).

Earlier researchers have found that due to the rotation of wheel, the viscous air present around also rotates and creates a sheath of air which prevents the lubricating fluid to reach into the grinding zone (Catai et al., 2006; Guo & Malkin, 1992; Mandal et al., 2010; Mandal, Majumdar, et al., 2011). The investigation differs from those who have found pressure of this air boundary layer around three different wheels, namely, bare grinding wheel, rexine-pasted grinding wheel and a cast iron solid wheel, in order to search the difference among those results and to find out reasons behind these differences to evaluate the strategy for better delivery of grinding fluid inside the grinding zone. Also in this finding, the generated data of these differences in boundary layer pressure among various wheels may help development of some flow model by future researchers. Earlier findings have generated data for grinding wheel only (Catai et al., 2008; Das, 2003; Mandal et al., 2010, 2012, 2013a, 2014; Mandal, Majumdar, et al., 2011; Mandal, Singh, et al., 2011; Ramesh et al., 2001). Catai et al. (2008) have found the speed and pressure generated around the grinding wheel. Mandal and others have also measured the flow of air around the grinding wheel (Mandal et al., 2012, 2013a, 2014;

Mandal, Singh, et al., 2011). In other investigations, Mandal and others have observed the air pressure around grinding wheel and rexine-pasted grinding wheel (Mandal et al., 2010; Mandal, Majumdar, et al., 2011). Das have also used the rexine cloth to control the flow of air (Das, 2003). Ramesh have also studied the characteristics of air curtain layer around grinding wheel and developed coolant shoe for better grinding fluid delivery to grinding zone (Ramesh et al., 2001).

This work is done to examine how the velocity profile of solid wheel differs from grinding wheel. The grinding wheel differs from solid wheel for its porosity due to the irregular shapes and orientation of grits and its surface has also some roughness compared to solid wheel. This study is to give another novel idea about the role played by the porosity and roughness of a grinding wheel in the formation of air boundary layer.

The finding of pressure close to wheel surface is not possible as axis of pressure measuring probe is not able to reach up to the grinding wheel surface due to its own diameter. Therefore, modelling becomes necessary (Mandal, Majumdar, et al., 2011; Jia, Li, & Li, 2013). This paper also suggests a model to quantify the pressure closer to the solid boundary of the wheel which otherwise is difficult to learn by practical experiment and which may be a valuable data to determine force of jet of cutting fluid at which it must fall on the wheel.

The present investigation has been carried out to suppress the air layer to a further extent by covering the side faces of grinding wheel by a thick rexine cloth and deflecting the air around the wheel by scraper board made of hard paperboard. These authors have already reported some early works done on rexine-pasted wheel (Mandal, Majumdar, et al., 2011). However, further efforts are made on the suppression of the air boundary layer by scraper board in all three types of wheels to learn the difference in rate of suppression of pressure around the grinding wheel, rexine-covered wheel and solid wheel along with scraper board. These data again are helpful in model built up to search the optimized condition for suppression of this hindering air layer in the impingement of coolant deep into the tool-work interface. Covering the grinding wheel by rexine cloth and using a scraper board along with are planned to compare air pressure obtained with that around the solid wheel. Finding the pressure difference experimentally, in all different conditions, between solid and grinding wheel when they rotate with the same angular velocity and finding the pressure adjacent to no-slip boundary is the novelty of this study. Percentage increase in pressure in case of grinding wheel compared to that in solid wheel and rexine-pasted wheel is measured that is new to its kind. Suppression of air pressure by scraper board in all three types of wheel is also noted. Formulating the effect of porosity and roughness of grinding wheel to augment the air boundary layer is original in nature. Models are made in three different methods to predict the pressure quite close to grinding wheel surface to find the air boundary layer pressure that is also unique.

2. Experimental conditions and procedure

A cast iron (CI) solid disc (Figure 1), alumina grinding wheel (Figure 2) and same grinding wheel covered with rexine cloth on both the faces (Figure 3) are considered for making a comparative study of air pressure around them. Typical shape of CI disc is given to reduce its weight. These three types of wheels are chosen to check the effect of pores and roughness of grinding wheel on the formation of air boundary layer around. By rexine cloth, all the pores on both the side faces of wheels are blocked and in solid wheel, the pores and surface roughness both are absent. A standard calibrated Prandtl-type Pitot tube along with U-tube manometer is utilized to measure air pressure. One end of the U-tube manometer is connected to Pitot tube and the other end is left open to the atmosphere. Water is used as manometric fluid. The least count for measuring air pressure using this set-up is 9.81 Pa and the coefficient of Pitot tube used is 0.983.

Initially, the probe (Pitot tube) is kept at 0–0 position as shown in Figure 4, and then moved in radial outward direction. Subsequently, this tube is positioned at five locations at left side of 0–0 position (considered as negative direction) and five locations at right side of 0–0 position (considered as

Figure 1. Cast iron disc.

Figure 2. Alumina wheel.

Figure 3. Rexine cloth covered alumina wheel.

positive direction) at an interval of 2 mm, and at each of these locations, Pitot tube is moved in radial outward direction. At successive 2 mm intervals in radial direction, air pressure is measured while the wheel rotates at 29.3 m/s velocity. It is continued till the deflection of water column in the manometer becomes zero. The dispersion of water column is measured in length unit and then converted to pressure. The probe is tried to place at nearest to the wheel periphery to obtain the value of air pressure as close as possible to the cutting surface. But as the outer diameter of it is 6.32 mm, the axis of pitot is possible to maintain at maximum 3.5 mm distance from wheel periphery. This procedure is followed for all three types of wheel selected here as described in Table 1.

Figure 4. Schematic representation of placing pitot tube and 0–0 position of wheel surface.

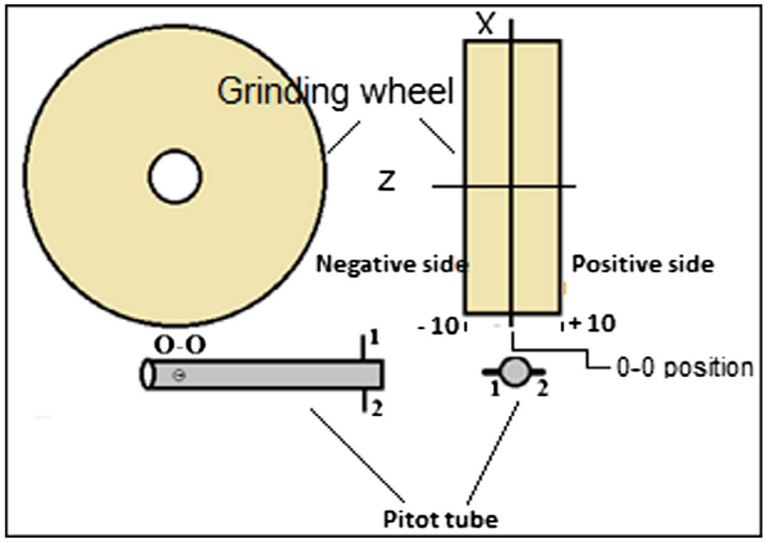

Table 1. Experimental set-up	
Machine	**HMT-Praga surface grinding machine, India**
	Model: 452P
Type of wheel	(a) Cast iron solid wheel
	Size: ϕ200 OD × 20 thk × ϕ31.75 mm bore
	(b) Grinding wheel
	Specification: AA46/54K5V8
	Size: ϕ200 OD × 20 thk × ϕ31.75 mm bore
	(c) Rexine pasted wheel
	Rexine of ϕ200 mm pasted on both the sides of wheel
Probe	Calibrated Prandtl-type pitot tube of size: ϕ6.32 mm OD

Figure 5. Positioning pitot tube and scraper board against grinding wheel.

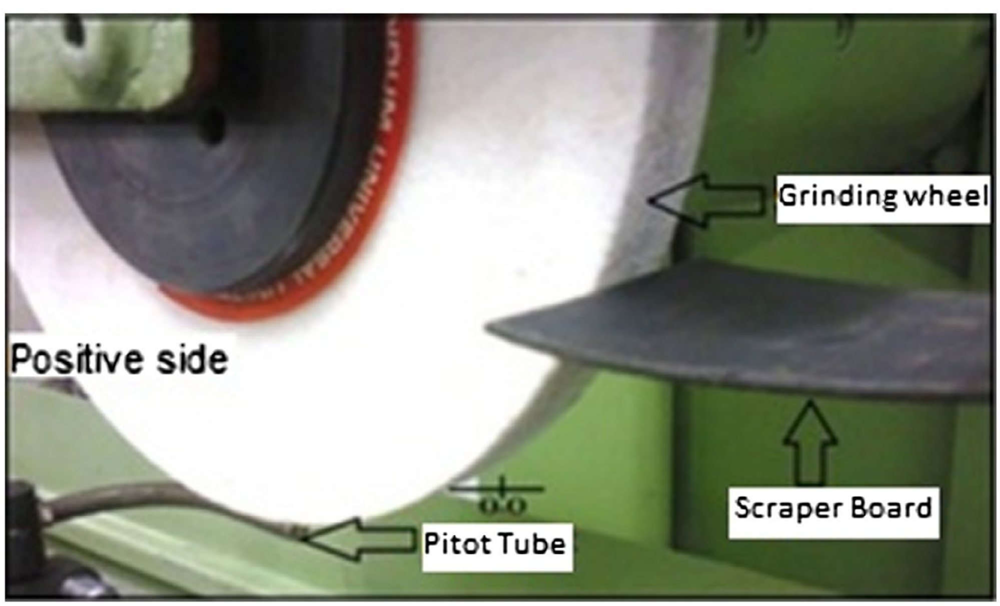

In another set of experiment, a PVC scraper board is used in intend to obstruct the air layer formed due to the rotation of wheel in static air. Arrangement of scraper board with wheel is shown in Figure 5. Conditions for experiments performed using grinding wheel are outlined in Table 2.

Further, a low alloy steel specimen is ground using the specified wheel with 20 μm infeed to explore improvement in grindability.

3. Results of comparative study of air pressure distribution pattern around solid disc, grinding wheel and rexine-pasted wheel

As the wheel rotates, a film of air around it also circulates due to its viscous effect (Massey, 2001; Shelly, Cashman, & Vermaat, 2007; White, 2005). Pressure of the rotating air is measured at constant velocity of wheel. Three types of wheels of same dimensions are selected in this study. This is to find out the pressure difference of air boundary layer around grinding wheel and rexine-pasted wheel to that of a solid wheel, if any, and to propose reasoning behind this which may lead to adopt the measures in order to increase the flow of grinding fluid inside the grinding zone. Pressure of this air film is measured at various radially outward locations corresponding to each width wise location of wheel. In width wise direction, measurement is made at an interval of 2 mm each. From each of these points, the pitot is moved at the succession of 2 mm in radial outward direction, for all the three wheels, and results obtained are shown in Figures 6–8. The axis of the pitot end is placed 3.5 mm away from wheel surface. Air pressure is found to decrease away from the wheel at radial direction. Near to the solid boundary, air layer pressure is quite large. It gets drastically lowered slightly away from wheel surface. It happens because the layer adjacent to wheel is carried away by wheel by viscous effect which gets gradually lessened away from the wheel surface. Figures 6–8 show the air pressure around three different wheels. It is obvious from those figures that the air pressure and boundary layer thickness of air is found to be maximum in grinding wheel, minimum in solid wheel, whereas rexine-covered wheel lies in between them. During rotation of grinding wheel, air leaves the wheel periphery due to centrifugal action. Low-pressure region is formed at two side

Figure 6. Variation of air pressure in radially outward direction and at various points along the thickness of grinding wheel.

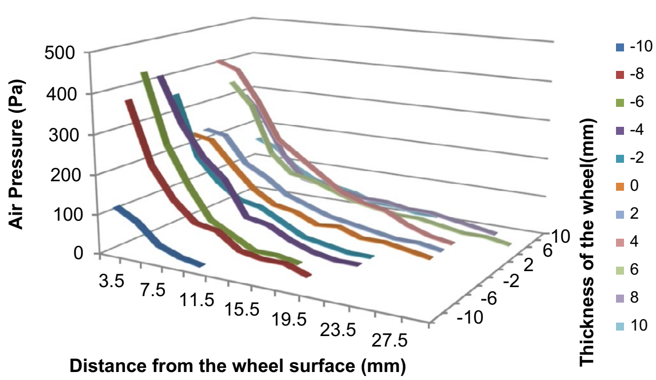

Figure 7. Variation of air pressure in radially outward direction and at various points along the thickness of rexine-pasted grinding wheel.

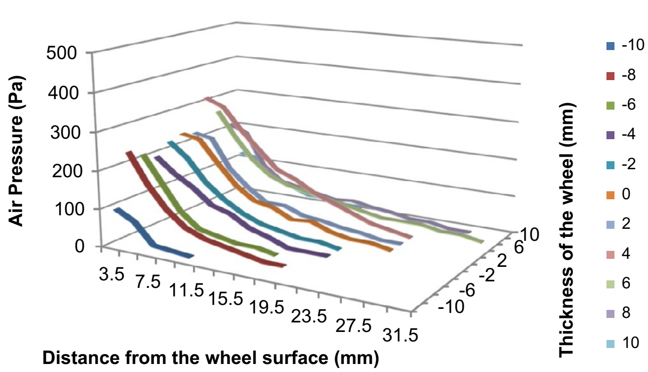

faces of the wheel. The wheel being porous in nature, suction of air takes place through the side faces. When the wheel rotates in air, air from both the sides rushes towards wheel periphery which is also at a low-pressure region. Covering those side faces by impermeable rexine cloth is, therefore, expected to reduce suction of air through these faces, and consequently, reduction of air pressure at the outer periphery is observed in Figure 7. In case of the solid CI disc, there is no question of porosity, and hence, there is no contribution of centrifugal effect of air through the disc. Sole reason for formation of air boundary layer surrounding the disc is, therefore, likely to be viscous effect of solid–fluid interaction. This results in low air layer pressure with this solid disc. In all the cases, air layer pressure is lesser at the outermost region of the wheel thickness, and it is higher at 4–6 mm inside the outermost points of wheel thickness. Typical air flow pattern around the faces and that around the wheel thickness and their interaction may have resulted in this variation of air pressure. Similar observations were also reported by others (Catai et al., 2006, 2008; Mandal, Majumdar, et al., 2011; Mandal, Singh, et al., 2011). The difference in air pressure generation on all the three types of wheels towards radial direction is shown in Figure 9.

The thickness of the wheel (20 mm) is divided in 10 equal divisions in the experiment. The extreme edge of the wheel facing the structure of the surface grinder is considered as −10, extreme edge of opposite side is considered as 10 and the centre of these two extreme edges is considered as 0–0 point (Figure 4). When observed in widthwise direction, the pressure profiles look similar in all three types of wheels though magnitudes are different. Increase in pressure is observed maximum near the 0-0 position and it decreases towards the edge of the wheel (Figure 10). However, little low-pressure region is found near the centre of thickness with comparison to the nearby outer region. All

Figure 8. Variation of air pressure in radially outward direction and at various points along the thickness of cast iron wheel.

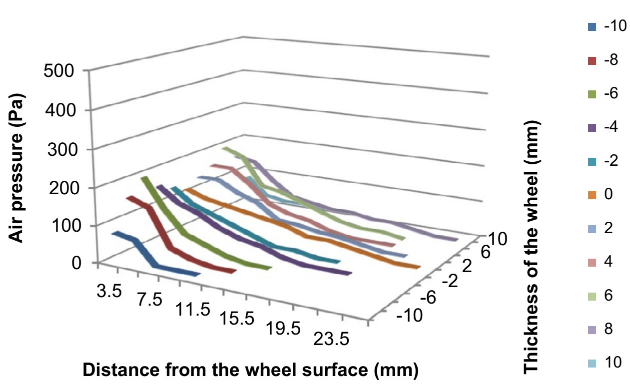

Figure 9. Variation of air pressure in radially outward direction at a width wise location 4 mm from 0–0 position.

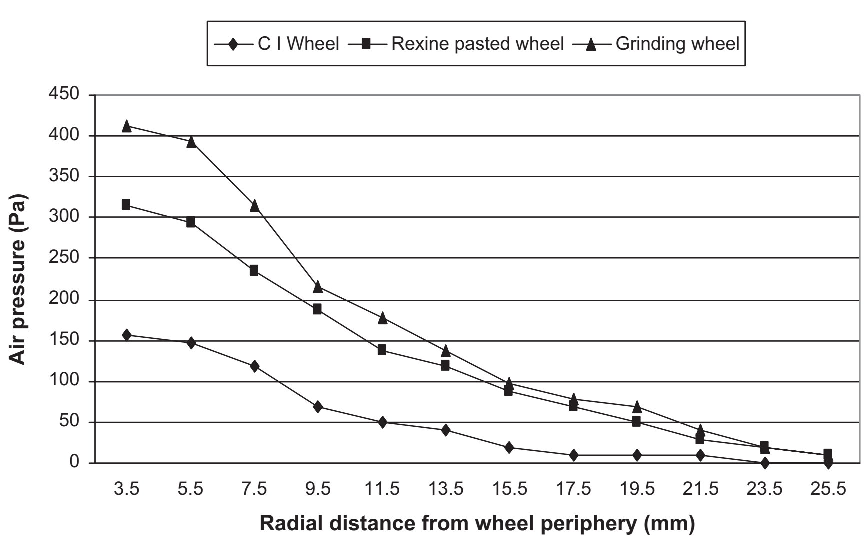

Figure 10. Comparison of air pressure measured along the width of the rotating wheel at a fixed distance from periphery.

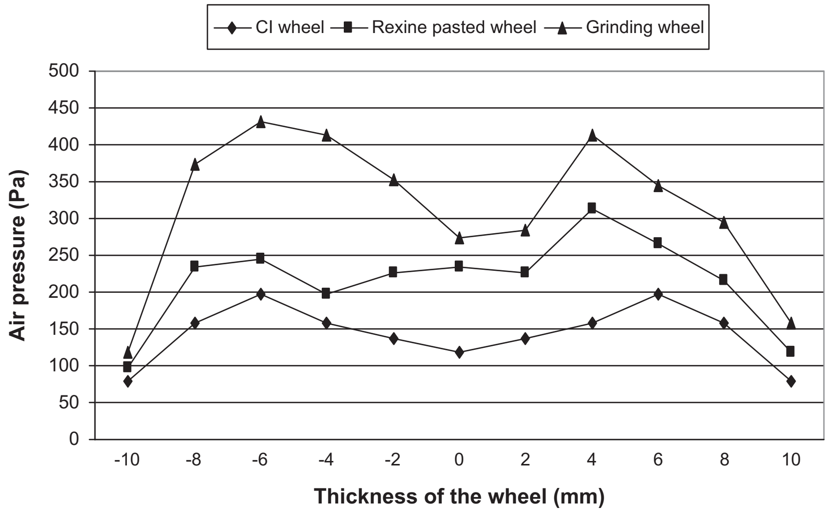

Figure 11. Percent increase in pressure in grinding wheel than that of solid wheel along the thickness of the wheel.

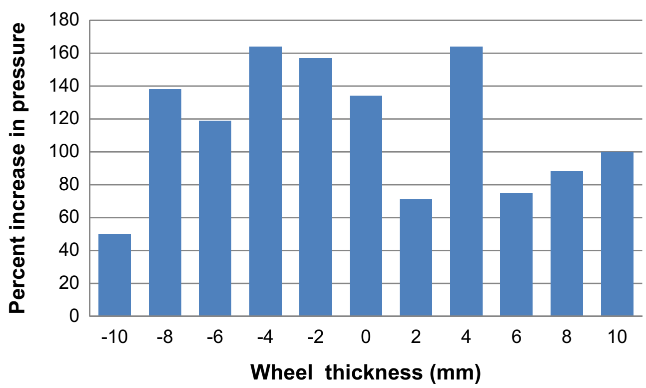

Figure 12. Percent increase in pressure in rexine pasting than solid wheel along the thickness of wheel.

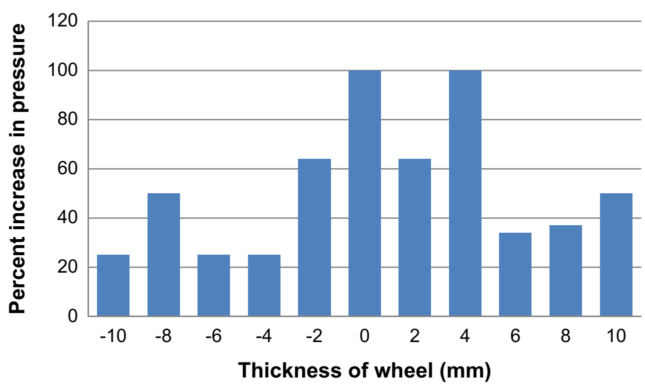

these profiles are found to be highly non-linear in nature. This shows the nature of pressure development around grinding wheel that is similar to other types of wheels when rotated in static fluid media. Two picks of pressure is found near two edges of all type of wheels. This may be due to the rushing of air through axial direction (Figure 4) towards the wheel when it rotates in air. But the peak at negative side is found higher than positive side (Figure 5) as in the flow of rotating air is somehow disturbed by the presence of wheel cover and the machine structure.

Figure 13. Variation of air pressure in radially outward direction and at various points along the thickness of grinding wheel with scraper board.

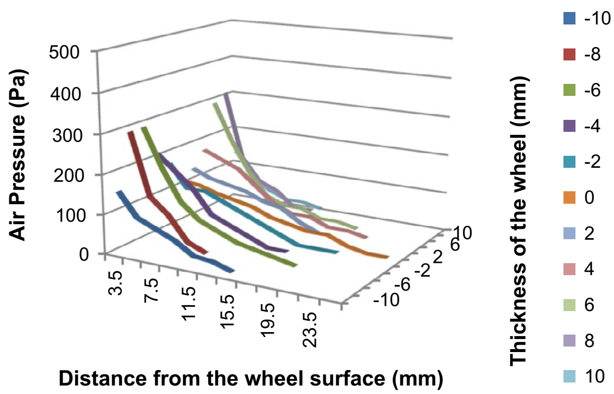

Figure 14. Variation of air pressure in radially outward direction and at various points along the thickness of rexine-pasted grinding wheel with scraper board.

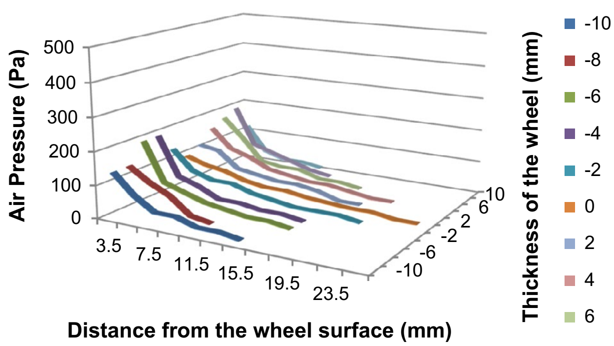

Figure 15. Variation of air pressure in radially outward direction and at various points along the thickness of cast iron wheel with scraper board.

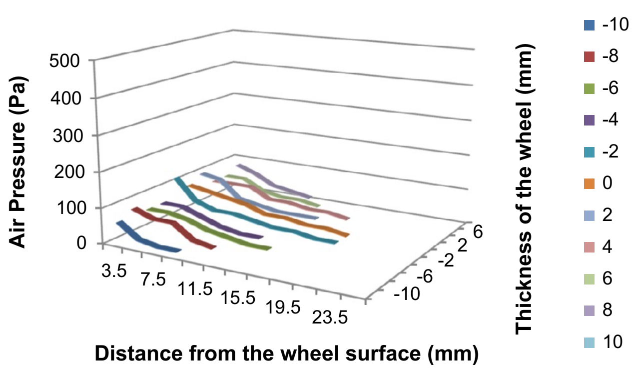

Least pressure is observed in solid wheel, whereas the rexine covered grinding wheel which seems to look like the solid wheel in nature as the pores on side faces of the wheel are closed by a rexine cloth shows a little increase in pressure than solid wheel (Figures 11 and 12). In case of grinding wheel, it is found maximum than other two wheels. It may be due to the reason that when wheel rotates in a static fluid, low pressure is created at the side faces in comparison to cutting face of wheel which ultimately leads to suction of air through that low-pressure region and which subsequently comes out through radial direction due to centrifugal action of air through pores of grinding wheel and enhance the pressure at high-pressure region further. Covering these side faces by pasting thick cloths may reduce this suction of air which results in decrease in pressure in case of rexine-pasted wheel than that of grinding wheel. Figure 12 demonstrates the quantification of increase in pressure in rexine-pasted wheel than a solid wheel. It ranges between 22 and 100%.

There is no centrifugal effect (Mandal, Majumdar, et al., 2011) of air in case of CI wheel. Therefore, centrifugal effect of porous wheel can be obtained by subtracting air pressure around solid wheel

Figure 16. Air pressure in radially outward direction at width wise 0-0 position with scraper board.

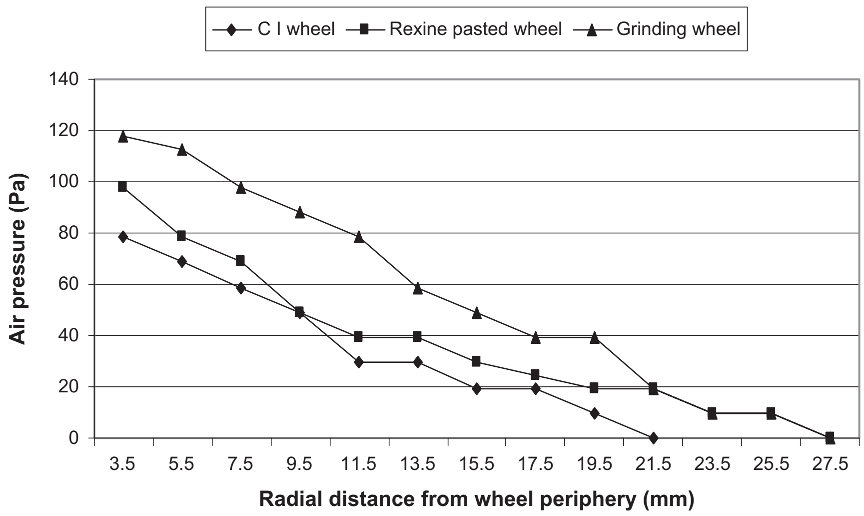

Table 2. Experimental conditions using grinding wheel	
Wheel surface velocity	29.3 m/s
Environment	Dry
Techniques used	1. Using a bare grinding wheel
	2. Use of rexine-pasted wheel
	3. Use of scraper board with bare grinding wheel
	4. Use of scraper board with rexine-pasted wheel

from that of grinding wheel. Increase in pressure around porous wheel periphery from that of solid wheel is in the range of 50–164% when measured at a position 3.5 mm away from wheel periphery. When observed widthwise, maximum increase in air pressure is found at a distance of 4 mm from the midpoint (0–0 position) of wheel thickness on both the sides. Near to the wheel surface, air velocity is maximum, and it reduces gradually with the distance from wheel periphery. This nature is found similar in all type of wheels.

Similar observation has been carried out by placing a scraper board, made of hard and thick paper, as shown in Figure 5. The width of the scraper board is taken more than the thickness of wheel, and is placed quite close, but without touching the abrasive grits of wheel. This is done to avoid the grinding of scraper board by grinding wheel against which it is placed. The intensity of pressure is found to be reduced to a further extent by breaking the air layer by this method (Figures 13–16). This happens due to the diversion of air seath which rotates along with the wheel, by a piece of scraper board. When this seath of rotating air is diverted, comparative low-pressure region is created after the scraper board, indicating the zone where delivery of grinding fluid has to be done for the better impingement deep inside the grinding zone. The experiments are carried out by keeping the scraper board 45° behind the opening of pitot tube along the wheel periphery (Figure 5). When scraper board is used with the rexine-pasted wheel, reduction of air pressure occurs in two ways (Figure 14). One way is by impeding suction of air through pasting side faces of grinding wheel by rexine cloth, so that centrifugal throw of air cannot reinforce the boundary layer much (Figures 3 and 7). Then the remaining air which rotates along the wheel due to viscosity is diverted physically by a scraper board. While experimenting with scraper board, the intensity of pressure and thickness of boundary layer is found to be lesser than that without using the scraper board as shown in Table 3. The reduction in average air pressure in rexine-pasted wheel at 3.5 mm radial distance from wheel peryphery is 30% and when rexine-pasted wheel is tested along with scraper board, 50% decrease in average air pressure is reported in comparison with the grinding wheel. Hence, maximum reduction of boundary air pressure can be possible with the combined use of scraper board and rexine cloth on a grinding wheel.

It is found almost 20% decrease in boundary layer for all types of wheels, whereas 37% lesser air pressure is found in rexine-pasted wheel when scraperboard is employed than without scraper board. The maximum range of boundary and the pick pressure is considered for quantifying the difference in Table 3.

While studying the air flow pattern width wise, the differences in air layer pressure in the wheels are observed at a radial distance of 3.5 mm. Porous wheel shows the maximum air pressure than that of the other two (Figure 17). The possible reason for formation of two picks may be that with the rotation of wheel, some low-pressure region may be generated near to circular periphery of the wheel which may cause surrounding air to rush towards that low-pressure region from axial direction of wheel, resulting in the development of those two picks. At negative side of thickness as shown in Figure 10, higher pressure is observed than positive side. It is because, the negative side of the wheel faces the structure of the surface grinding machine on which all the tests are carried out. For rexine-covered wheel, axial suction of air through its pores is restricted (Figures 7 and 14). However, mainly roughness of surface due to the irregular orientation of grits causes its profile to stay above the profile of solid wheel.

When scraper board is used to break this ring of stiff air, much reduced value of air pressure is observed as shown in Figure 17. But the profile observed here is also similar to Figure 10 but with lower magnitude. Figure 18 portrays the percentage increase in pressure in grinding wheel than rexine-pasted wheel. When pores on the sides of the grinding wheel are covered, suppression of air layer is found possible by nearly 28%. But when both, wheel is covered and scraper board is used, diminishes the pressure by nearly 51% (Figure 19). Hence, the use of scraper board along with the

Table 3. Percent decrease in boundary layer thickness and air pressure around the wheels with the employment of scraper board than without scraper board

Percent decrease in boundary layer			Percent decrease in air pressure		
Grinding wheel	Rexine-pasted wheel	Solid wheel	Grinding wheel	Rexine-pasted wheel	Solid wheel
20	20	23	27	37	25

Figure 17. Comparison of pressure of stiff air layer around rotating wheel at a constant distance from wheel periphery using scraper board.

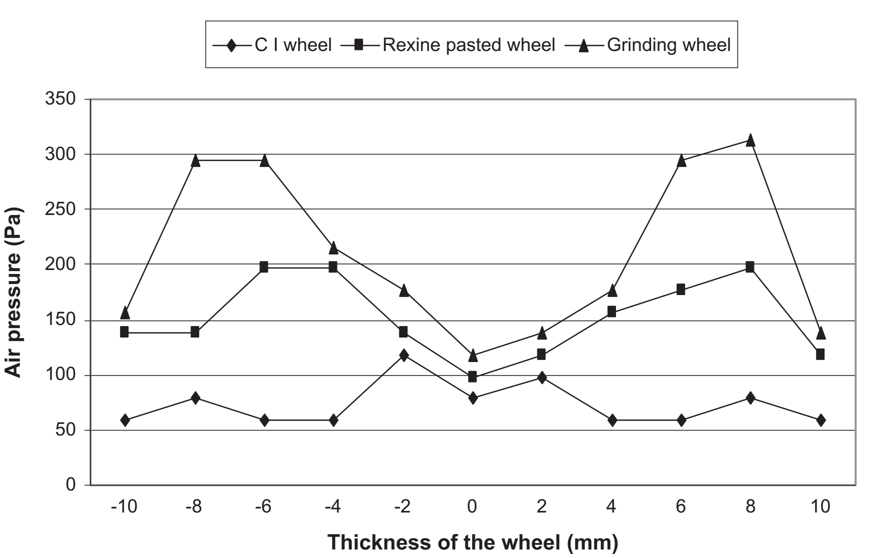

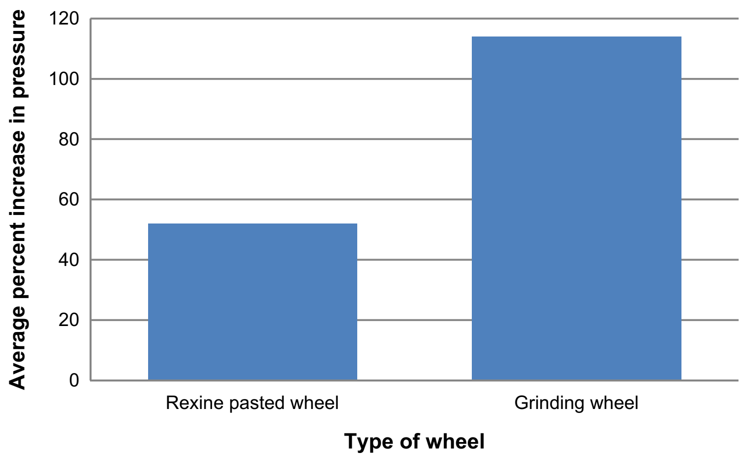

Figure 18. Average percentage increase in pressure in different wheels with comparison to solid wheel.

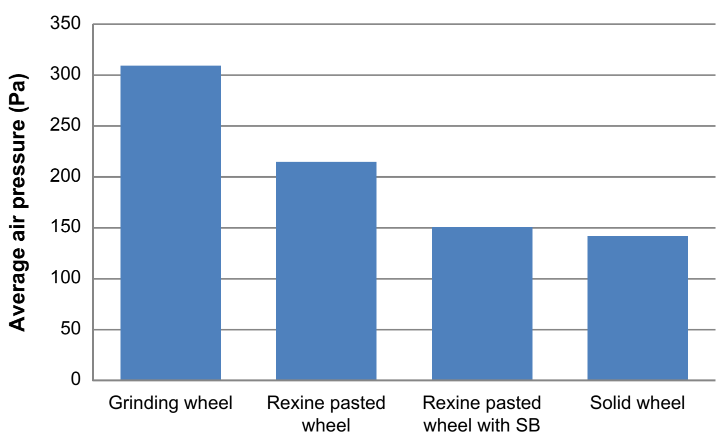

Figure 19. Average air pressure in various types of wheel and condition.

rexine-covered wheel can be considered to be more effective to promote better fluid delivery inside grinding zone. Use of rexine-covered wheel along with scraper board arrangement shows the reduction of the air boundary layer to a further extent, and very close to solid wheel when measured at a point behind and close to the scraper board (Figure 19) and better than the use of pneumatic barrier (Mandal et al., 2013a) because more than the 50% suppression is possible with this and is also less expensive. More investigations are required for further reduction of this boundary layer and how much cutting fluid delivery increases into the mating point of wheel and work-surface with the use of covered wheel and scraper board is also required to be quantified.

4. Effect of porous and rough wheel surface on air boundary layer

From Figures 17 and 19, it is obvious that pressure around grinding wheel is more than solid wheel and rexine-covered wheel. As the suction of air takes place through both the side faces of grinding wheel, as discussed early, and strengthens the air boundary layer, can be prevented by closing those pores by pasting impermeable cloth on both faces of grinding wheel. As suction of air is stopped by covering the sides of grinding wheel, the manometer reading will be less in this wheel than that of grinding wheel. So, comparison of average pressure of grinding wheel and rexine-pasted wheel reveals that availability of small pores due to the random orientation and sizes of grits inside the grinding wheel contributes towards strengthening of air boundary layer (Figure 18). Therefore, pressure contributed by suction of air through pores can be found out by deducting pressure around rexine-covered wheel from the pressure around grinding wheel. So, effect of porosity (Ø) can be expressed as

$$Ø = \frac{P_g - P_r}{P_g} \times 100\% \tag{1}$$

In the experimented wheel, the value of porosity effect comes 30% of pressure value of grinding wheel.

When the same alumina wheel is covered with cloth, suction of air through its side faces and driving out of the same through cutting edges of wheel due to centrifugal effect is ruled out like solid wheel. But in experiment, pressure around rexine-covered wheel is found to be more than solid disc (Figure 19). This may be attributed to the roughness at cutting surface of the wheel due to the uneven orientation of cutting edges of abrasive grits. Therefore, effect of roughness (ρ) can be expressed as

$$\rho = \frac{P_r - P_s}{P_r} \times 100\% \tag{2}$$

where P_g is the pressure around grinding wheel, P_r is the pressure around rexine-covered wheel and P_s is the pressure around solid wheel.

The value of roughness effect in the experimented wheel comes 33% of pressure around rexine-pasted wheel.

5. Modelling air boundary layer pressure

By experimental method, finding out of pressure closure to surface, after no-slip boundary, becomes difficult due to physical constraints of practical experiments. Due to this, the axis of Pitot tube which is used for measuring pressure is kept at 3.5 mm away from the rotating wheel surface as the diameter of it is 6.32 mm and to avoid the grinding of it. Therefore, the air pressure at that zone (from wheel surface to 3.5 mm distance radially outward) is unaddressed in practical investigation, finds the inevitability of extrapolation of data obtained from practical experiments. Speed of the wheel is taken as boundary condition while forecasting the pressure closure to wheel surface.

In this paper, extrapolations of the curves are examined by three different methods, namely, Trend Line, Origin Pro and Trend Function. Preparation of trend models is a very simple method and

Table 4. Estimated values by three different methods and errors

Position of the probe along the width of wheel from position (mm)	Experimented air pressure value at x = 3.5 mm (a)	Air pressure value by trend line method at x = 3.5 mm (b)	Square of the error $[(b - a)]^2$	Air pressure value by origin pro at x = 3.5 mm (c)	Square of the error $[(c - a)]^2$	Air pressure value by trend function method at x = 3.5 mm (d)	Square of the error $[(d - a)]^2$
2	235	113	14,884	294	630	294	630.01
4	412	232	32,400	471	204.49	470	196
6	343	145	39,204	412	404.01	412	404.01
8	294	−1,394	2,849,344	333	174.24	333	174.24
10	156	69	7,569	186	368.64	186	368.64
0	274	228	2,116	334	475.24	333	462.25
−2	353	138	46,225	255	767.29	255	767.29
−4	412	190	49,284	373	88.36	372	94.09
−6	431	125	93,636	354	316.84	353	324
−8	372	111	68,121	293	449.44	294	400
−10	117	24	8,649	137	289	137	289
MSE			291,948.4		3,745.7		3,731.6

is used by researchers for various technical analyses which basically represent a model from simple regression analysis for predicting the value of dependent variable from independent variable. Many types of trend models are in use. A linear model is best for the data-sets which are simple linear but cannot be used effectively when the data changes in non-linear way. Logarithmic curve is most useful when the data initially changes quickly and then levels out. Polynomial model is suitable for fluctuating data-set. Power trend model is used for the data-set which increases at a specific rate. Moving average method does smoothening of fluctuations in data. It uses a specific number of data points, averages them, and uses the average value as a point in the trend line. But Exponential method finds the trend suitably when the data value increases or fall at increasingly higher rate (Arsham & Shao, 1985; Jelen, 2010; Jha, Sinha, Arkatkar, & Sarkar, 2013; Shelly et al., 2007).

Trend function calculates the required trend line through a given set of *y*-values and (optionally) a given set of *x*-values. It first trains the previously obtained last two values. The function then extends a trend line by taking tangent from previous trained data to calculate additional set of *y*-values for a further supplied set of new *x*-values (http://www.excelfunctions.net/Excel-Trend-Function.html). Origin Pro of Origin Lab also does the extrapolation to estimate beyond experimental observations corresponding to the gradients obtained from previous data.

Extrapolations are carried out to find the value of air pressure at the surface of wheel periphery, beyond the range of experiment, which is necessary to build a strategy of issuing grinding fluid jet into the tool-work interface. But it is also obligatory to find the method by which the error of estimation is minimal. Therefore, extrapolation has been carried out by all determined methods and checked for percentage of error with respect to experimentally obtained values. The method which can show the minimum value of error should be considered for making model. The experimental value closest to the wheel periphery was obtained at 3.5 mm ($x = 3.5$ mm) away from it. Other values are taken at 2 mm succession from it and up to 25.5 mm. So, the curves obtained by taking the pressure data at 5.5 mm to 25.5 mm are extrapolated by all methods to get the data at $x = 3.5$ mm. Then, these extrapolated data are to be matched with the experimented value, and Mean Square Error (MSE) is calculated in each case (Table 4) following the relation given below.

$$\mathrm{MSE} = \frac{1}{N}\sum_{i=1}^{N}\left[E_{\mathrm{est}} - E_{\mathrm{exp}}\right]^2$$

where E_{est} stands for a vector of estimated value and E_{exp} represents a vector of experimented value.

From Table 4, it is found that the Trend Line value gives the maximum error. But MSE of Trend Function value (3,731.6) shows marginally better results than estimated data obtained by Origin Pro (3,745.7). Therefore, values obtained by Trend Function are considered for this work to estimate the air pressure at $x \approx 0$. The pressure thus obtained is shown in Table 5.

The estimated values give the air pressure adjacent to the grinding wheel surface that is plotted in Figure 20. These obtained values by Trend Function method having minimal error, is chosen for taking the basis for building model using MATLAB software. The model is built up on the basis of the plot fabricated by the values estimated by Trend Function method. Model is selected on the basis of MSE which are shown in Table 6. Minimum MSE gives the maximum accuracy. Various polynomials have been attempted, but 7th degree polynomial is found to give the minimum value of MSE, 2,370.032 (Table 6), with respect to estimated value as given in Table 5. Therefore, it is preferred over other types of polynomials (Figure 20). It shows a pretty good match with the estimated curve.

The empirical relation obtained for the model to obtain the value of pressure at any point along the thickness of the grinding wheel is given as:

$$y = 0.00032x^7 + 0.00065x^6 - 0.057x^5 - 0.22x^4 + 3.3x^3 + 14x^2 - 77x + 3.6\times10^2$$

Table 5. Estimated value of air pressure adjacent to grinding wheel periphery

Position of the probe along the width of wheel from position (mm)	Estimated reading at x ≈ 0 mm by trend function method (Pa)
0	309.01
2	252.6
4	446.35
6	446.35
8	397.3
10	191.29
−2	627.84
−4	618.03
−6	740.65
−8	647.46
−10	169.2

Figure 20. Model and experimented curve of boundary layer pressure along the thickness of the wheel.

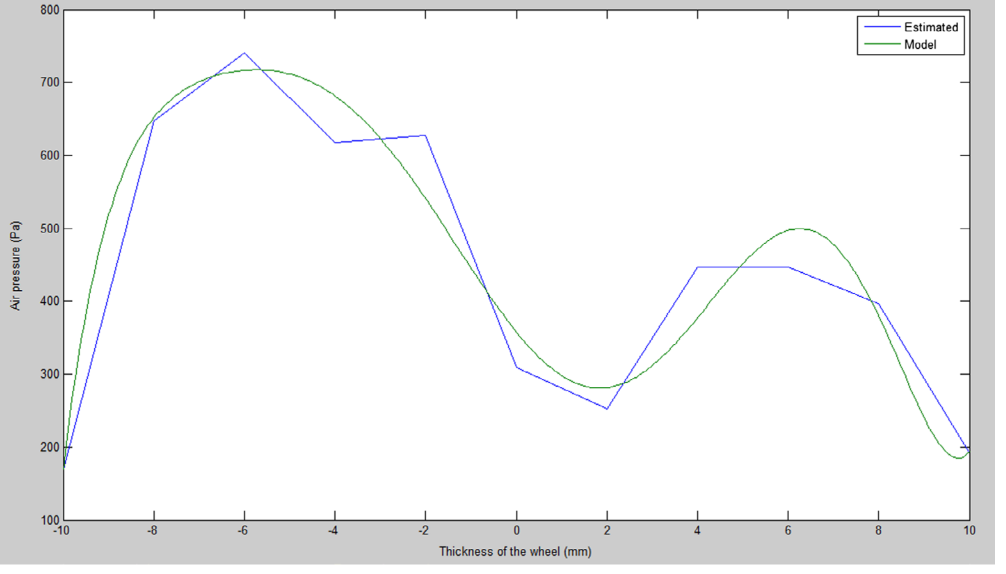

Table 6. Values of mean square error (MSE) for modelling air pressure by different polynomials

Order of polynomials	MSE
2nd	25,246.71
3rd	18,498.42
4th	3,394.044
5th	3,337.027
6th	3,195.396
7th	2,370.032
8th	2,803.117
9th	40,475.36
10th	23,41635

where *x* is the input data (distance along the width of wheel) and *y* is the predictive response (boundary layer pressure).

The model observed in Figure 20 is found to give a good fit to the experimental result with respect to the purpose for which it is prepared. Two picks are observed in the model near to the outer surface of the wheel. When a wheel rotates, air around it also rotates to satisfy the no slip condition. Due to centrifugal effect, the air around leaves the wheel periphery and the air from both the sides of the wheel then rush to fill the gap and may collide to give rise of two picks as seen in Figure 20. The pick at the left side is more due to the presence of irremovable wheel cover at that side and structure of the surface grinder machine on which the wheel is fitted.

This relation can be used to find the boundary layer pressure at any point along the thickness of the wheel without going on to experiment for the given grinding wheel that, in turn, may help to select the appropriate condition for applying grinding fluid in sequence to decrease grinding temperature.

6. Conclusions

Following conclusions can be made from the present experimental investigation:

(1) Pressure around the grinding wheel is measured to be quite high than that of the rexine-pasted wheel and solid CI disc. In comparison with the solid disc, air pressure around the grinding wheel is found to be higher by 50–164%.

(2) Air pressure is observed to get suppressed by 3.5–53% with the use of rexine-pasted wheel. On the other hand, pressure of air layer is reduced by a maximum of 57% near to the centre of wheel width with the use of scraper board. Therefore, rexine-pasted wheel along with scraper board is found out to be more effective in the present work.

(3) Due to porosity in grinding wheel pressure increases by 30% and due to roughness, it is 33%. Effect of roughness may not be avoided but porosity-effect can be reduced by rexin-pasted wheel.

(4) Air flow can be modelled by Trend Function and can give higher precision value near to the wheel surface by which the pressure required to issuing grinding fluid jet can be determined.

Acknowledgment
Required facilities to carry out the work have been provided by Kalyani Government Engineering College, Kalyani.

Funding
The author received no direct funding for this research.

Author details
Sujit Majumdar[1]
E-mail: sujitmajumdar2010@gmail.com
Ahin Banerjee[2]
E-mail: ahin49banerjee@gmail.com
ORCID ID: http://orcid.org/0000-0002-2873-874X
Santanu Das[3]
E-mail: sdas.me@gmail.com
ORCID ID: http://orcid.org/0000-0001-9085-3450
Samik Chakroborty[4]
E-mail: chakrasamik@gmail.com
ORCID ID: http://orcid.org/0000-0002-0159-4440
[1] Department of Mechanical Engineering, Global Institute of Management & Technology, NH-34, Palpara More, Nadia, Krishnanagar 741102, West Bengal, India.
[2] Department of Mechanical Engineering, Indian Institute of Technology (BHU), Varanasi, Varanasi 221005, Uttar Pradesh, India.
[3] Department of Mechanical Engineering, Kalyani Government Engineering College, Kalyani 741235, West Bengal, India.
[4] Indian Maritime University, Kolkata Campus, P 19, Taratala Road, Kolkata 700088, India.

Citation information
Cite this article as: Experimental investigation and modelling on air layer formation around a rotating grinding wheel, Sujit Majumdar, Ahin Banerjee, Santanu Das & Samik Chakroborty, *Cogent Engineering* (2016), 3: 1183273.

Cover image
Source: Authors.

References

Akiyama, T., Shibata, J., & Yonetsu, S. (1984). Behavior of grinding fluid in the gap of the contact area between a grinding wheel and a workpiece. In *Proceedings of the Fifth International Conference on Production Engineering* (pp. 55–57). Tokyo.

Arsham, H., & Shao, S. P. (1985). Seasonal and cyclic forecasting for small firm. *American Journal of Small Business, IX*, 46–57.

Banerjee, S., Ghosal, S., & Dutta, T. (2008). Development of a simple technique for improving the efficacy of fluid flow through the grinding zone. *Journal of Materials Processing Technology, 197*, 306–313. doi:10.1016/j.jmatprotec.2007.06.045

Brinksmeir, E. (1993). High performance surface grinding–the influence of coolant on the abrasive process. *Annals of the CIRP, 42*, 367–370. doi:10.1016/S0007-8506(07)62463-9

Catai, R. E., Bianchi, E. C., Zilio, F. M., Valarelli, I. D. D., Alves, M. C. D. S., & Silva, L. R. D. (2006). Global analysis of aerodynamics deflectors efficiency in the grinding

process. *Journal of the Brazilian Society of Mechanical Sciences and Engineering, 28*, 140–145. doi:10.1590/S1678-58782006000200002
Catai, R. E., Silva, L. R. D., Bianchi, E. C., Aguiar, P. R. D., Zilio, F. M., Valarelli, I. D. D., & Salgado, M. H. (2008). Performance of aerodynamic baffles in cylindrical grinding analyzed on the basis of air layer pressure and speed. *Journal of the Brazilian Society of Mechanical Sciences and Engineering, 30*, 47–50. doi:10.1590/S1678-58782008000100007
Das, S. (2003). Improving grinding performance through appropriate grinding fluid application. In *Proceedings of the National Conference on Investment Casting* (pp. 97–103). Durgapur.
Ebbrell, S., Wooly, N. H., Tridimas, Y. D., Allanson, D. R., & Rowe, W. B. (2000). The effect of cutting fluid application methods on the grinding process. *International Journal of Machine Tools and Manufacture, 40*, 209–223. doi:10.1016/S0890-6955(99)00060-7
Guo, C., & Malkin, S. (1992). Analysis of fluid flow through the grinding zone. *Transactions of the ASME, Journal of Engineering for Industry, 114*, 427–434. doi:10.1115/1.2900694
Han, Z. L., & Li, C. H. (2013). Theoretical modeling and simulation of airflow field near grinding wheel. *International Journal of Control and Automation, 6*, 145–155.
Jelen, B. (2010). *Creating Microsoft Excel charts that show trends*. Indianapolis, IN: QUE.
Jha, K., Sinha, N., Arkatkar, S. S., & Sarkar, A. K. (2013). Modeling growth trend and forecasting techniques for vehicular population in India. *International Journal for Traffic and Transport Engineering, 3*, 139–158. doi:10.7708/ijtte.2013.3(2).04
Jia, D.,Li, C., & Li, R. (2013). Modeling and experimental investigation of the flow velocity field in the grinding zone. *International Journal of Control and Automation, 7*, 405–416. http://dx.doi.org/10.14257/ijca.2014.7.2.36
Kovacevic, R., & Mohan, R. (1995). *Effect of high speed grinding fluid on surface grinding performance* (SME Technical Paper, MR 95-213, pp. 919–931). Dearborn.
Malkin, S. (1990). *Grinding technology: Theory and application of machining with abrasives*. Chichester: Ellis Harwood.
Massey, B. (2001). *Mechanics of fluid* (7th ed.). Cheltenham: Nelson Thornes.
Majumdar, S., Mandal, B., Das, S., & Chakroborty, S. (2015). Modeling air layer pressure around a rotating grinding wheel. *Global Journal on Advancement in Engineering and Science, 1*, 56–63.
Mandal, B., Biswas, D., Sarkar, A., Das, S., & Banarjee, S. (2013a). Improving grindability of inconel 600 using alumina wheel through pneumatic barrier assisted fluid application. *Advanced Materials Research, 622–623*, 394–398. doi:10.4028/www.scientific.net/AMR.622-623.394-&gt
Mandal, B., Biswas, D., Sarkar, A., Das, S., & Banarjee, S. (2013b). Grinding performance using a compound nozzle characterised by small discharge of fluid. *Journal of the Association of Engineers, India, 83*, 28–35.
Mandal, B., Das, G. C., Das, S., & Banerjee, S. (2014). Improving grinding fluid delivery using pneumatic barrier and compound nozzle. *Production Engineering Research and Development, 8*, 187–193. doi:10.1007/s11740-013-0507-x
Mandal, B., Majumdar, S., Das, S., & Banarjee, S. (2010). Predictive modelling and investigation on the formation of stiff air layer around the grinding wheel. *Advanced Materials Research, 83*, 654–659. doi:10.4028/www.scientific.net/AMR.83-86.654
Mandal, B., Majumdar, S., Das, S., & Banerjee, S. (2011). Formation of a significantly less stiff air layer around a grinding wheel pasted with rexine leather. *International Journal of Precision Technology, 2*, 12–20. doi:10.1504/IJPTECH.2011.038106
Mandal, B., Singh, R., Das, S., & Banerjee, S. (2011). Improving grinding performance by controlling air flow around a grinding wheel. *International Journal of Machine Tools and Manufacture, 51*, 670–676. doi:10.1016/j.ijmachtools.2011.06.003
Mandal, B., Singh, R., Das, S., & Banerjee, S. (2012). Development of grinding fluid delivery technique and its performance evaluation. *Materials and Manufacturing Processes, 27*, 436–442. doi:10.1080/10426914.2011.585487
Morgan, M. N., Jackson, A. R., Wu, H., Baines-Jones, V., Batako, A., & Rowe, W. B. (2008). Optimisation of fluid application in grinding. *CIRP Annals-Manufacturing Technology, 57*, 363–366. doi:10.1016/j.cirp.2008.03.090
Nguyen, T., & Zhang, L. C. (2006). The coolant penetration in grinding with a segmented wheel- part 2: Quantitative analysis. *International Journal of Machine Tools & Manufacturing, 46*, 114–121. doi:10.1016/j.ijmachtools.2005.05.020
Peukart, W. (2004). Material properties in fine grinding. *International Journal of Mineral Processing, 74*, 3–17. doi:10.1016/j.minpro.2004.08.006
Ramesh, K., Yeo, S. H., Zhong, Z. W., & Sim, K. C. (2001). Coolant shoe development for high efficiency grinding. *Journal of Material Processing Technology, 114*, 240–245. doi:10.1016/S0924-0136(01)00620-3
Schumack, M. R., Chung, J. B., Schultz, W. W., & Asibu, E. K., Jr (1991). Analysis of fluid flow under a grinding wheel. *Journal of Engineering for Industry, 113*, 190–197. doi:10.1115/1.2899677
Shelly, G., Cashman, T. J., & Vermaat, M. (2007). *Microsoft office 2007: Post-advanced concepts and techniques*. Boston, MA: Cengage Learning.
White, F. M. (2005). *Viscous fluid flow* (3rd ed.). New York, NY: McGraw-Hill.